J. agric. Engng Res. (2000) **75,** 257–264
doi:10.1006/jaer.1999.0501, available online at http://www.idealibrary.com on IDEAL®

Vehicle Guidance Parameter Determination from Crop Row Images using Principal Component Analysis

F. A. C. Pinto[1]; J. F. Reid[2]; Q. Zhang[2]; N. Noguchi[3]

[1] Department of Agricultural Engineering, Federal University of Viçosa, Viçosa, MG, 36571-000, Brazil; e-mail: facpinto@mail.ufv.br
[2] Department of Agricultural Engineering, University of Illinois at Urbana-Champaign, Urbana, IL 61801, USA; e-mail: j-reid1@sugar.age.uiuc.edu
[3] Department of Agricultural Engineering, Hokaido University, Sapporo 060, Japan; e-mail: noguchi@bpe.agr.hokudai.ac.jp

(Received 2 February 1999; accepted in revised form 16 October 1999)

An image recognition algorithm has been developed as part of a vision-based guidance system for row crops. Each combination of the vehicle guidance parameters, offset and heading angle, was treated as a 'pose' of the interested object, the crop rows. Whilst several pose recognition algorithms have previously been developed, the proposed algorithm is capable of determining the heading angle and the offset of a vehicle relative to the crop rows. A set of poses was collected and used as a training set. The training stage of the algorithm used the principal component analysis (Hotelling transform) to produce a low-dimensional eigenspace on which each pose was represented by its projections. Given a new image, the pose (heading angle and offset) recognition was done by projecting the image onto the eigenspace and determining the closest training image projection. Another set of poses was used to test the performance of the algorithm. Using different region of interest to train and test the algorithm, it presented the least average absolute error of 4·47 cm and 1·26° for offset and heading angle, respectively, when using the central part of images for pose determination.

© 2000 Silsoe Research Institute

1. Introduction

For many years, researchers have investigated autonomous guidance systems for agricultural vehicles. Research has been motivated by the potential improvements that will result by using automation technology. Autonomous vehicles have been suggested as a technological solution to a declining agricultural workforce (Noguchi *et al*., 1997) and to prevent operator mistakes due to the steering fatigue (Slaughter *et al*., 1997). Even partially autonomous guidance systems are perceived as beneficial for eliminating fatigue from redundant operations and for eliminating missed areas of the field by controlling application of seeds, fertilizers, water, pesticides, *etc*. (Tillet, 1991).

Tillet (1991) classified guidance systems as mechanical, optical, radio navigation, ultrasonic or leader cables system. Although each system uses different technologies to guide the vehicle, most of the systems use the same guidance parameters, heading angle and offset of the vehicle, to control the vehicle steering. Offset is the displacement of the vehicle gravity centre departure from the desired path. Heading angle is the angle between the vehicle centreline and the desired path. Owing to the technical limitations of each type of sensor, a robust guidance system may rely on a redundant sensing system, *i.e*. a multi-sensor integration approach (Noguchi *et al*., 1998b).

A vision system provides information not available from the other guidance sensors. For example, a vision system can extract other important information such as the crop health (Ahmad & Reid, 1996), the presence or level of weed infestation (Steward & Tian, 1998), the plant population and the stage of development (Noguchi *et al*., 1998a). This information has value within the context of the site-specific crop management. Thus, the flexibility of the vision system makes it a valuable sensor for agricultural process automation.

Previous research has addressed the influence of the video sensor inclination (tilt angle) on the overall accuracy of the system (Gerrish *et al*., 1987). A large tilt favours the offset determination since a field of view

closer to the vehicle is obtained. Thus, it can be supposed that using a fixed tilt angle, an analysis on the bottom part of the image favours offset determination while the top part favours the heading angle determination. A split image approach utilized this concept for foam marker tracking (Von Qualen *et al*., 1991).

Several image-processing algorithms have been proposed to extract the guidance parameters from crop row images (Reid, 1987; Billingsley & Schoenfish, 1997; Slaughter *et al*., 1997). These algorithms usually depend on crop row detection and some additional information about the geometry and position of the sensor to extract the guidance parameters. In this research, an algorithm that depends on fewer variables was developed by treating guidance parameter determination as a 'pose recognition' problem. The characteristic objects from the images are the crop rows and the 'pose' is the combination of offset and heading angle that produces images of crop rows from a fixed perspective.

Generally, this approach requires a large number of poses to represent the guidance signal. However, given that the images are of the same object with only slight changes in the pose, it is assumed that the set of pose images is correlated. This enables the use of coding techniques to compress the set of images into a lower-dimensional space.

Hotelling (1933) proposed a technique to decrease the number of vectors in a space basis. If such a space is represented by 'statistical variables x_1, x_2, …, x_n', the author proposed: 'The x's will ordinarily be correlated. It is natural to ask whether some more fundamental set of independent variables exists, perhaps fewer in number than the x's, which determine the values the x's will take'. Hotelling named his technique 'the method of principal components'. Today, principal component analysis (PCA) is also known as the Hotelling or Karhunen–Loeve transform (Gonzalez & Woods, 1992) and has been widely used in image processing field.

Turk and Pentland (1991) used PCA to develop a complete automatic face recognition system using a set of face images (the training set) to generate a lower-dimensional eigenspace by running a PCA routine. When a new image was input into the system, a decision process determined whether it was a face by using a threshold distance value from the image and the eigenspace. If the image was identified as a face image, it was classified as either a 'known face' or a 'new one' based on the threshold value of the distance between its projection and the training set image projections onto the eigenspace. If a random image was not a 'known face', the PCA routine was used to add the new face to the data set. The system achieved a performance that varied from 64 to 100% of correct classification depending on the lighting variation, face orientation, image size and threshold values used.

Murase and Nayar (1995) addressed the problem of recognition and pose estimation of three-dimensional objects from its appearance by using PCA to build a parametric eigenspace. They used a set of different images for each object of interest to generate a manifold (projections onto the eigenspace) that was parameterized by object pose and illumination. In order to recognize the object pose, they used the distance between the input image projection and the manifold points. The system used two eigenspaces to accomplish its task. The first, a universal eigenspace, was used to identify the object. The second one, the object eigenspace, was then used to recognize the object pose.

2. Objectives

The primary objective of the present work was to develop and test an algorithm to output the guidance parameters, offset and heading angle, by using principal component analysis to approach the task as a pose determination problem in an image. The influence of the region of interest used to compute the pose was studied as a secondary objective.

3. The principal component analysis

The objective of the principal component analysis (PCA) is to transform one set of random variables into another set of variables (components) which, although expected to be fewer in number than the original set, could adequately represent the original set (Hotelling, 1933). Principal component analysis has been used to solve a wide variety of problems and has experienced a number of different variations (Jolliffe, 1986). For instance, one PCA variation is used to find among the variables which ones best represent or classify an original set of data (Isebrands & Crow, 1975). Another PCA variation can look for a subspace, spanned by a fewer number of vectors than the original space, where the features of the original set can be adequately represented (Kirby & Sirovich, 1990).

As a transformation problem, PCA computes the eigenvectors of the covariance matrix of the original set of variables and uses them as a basis of a subspace that could represent the original set of variables. The sample covariance matrix R is defined by

$$R = \frac{1}{N-1} \sum_{i=1}^{N} (\mathbf{x}^{(i)} - \boldsymbol{\mu})(\mathbf{x}^{(i)} - \boldsymbol{\mu})^T = \frac{1}{N-1} XX^T \quad (1)$$

where $\mathbf{x}^{(i)}$ is the ith statistical vector variable, $\boldsymbol{\mu}$ is the mean vector, N is the number of variables $\mathbf{x}^{(i)}$ and X is

the matrix whose columns are the $(\mathbf{x}^{(i)} - \boldsymbol{\mu})$ vectors (the superscript T represents the transpose vector or matrix). Then, if each variable is a vector with dimensional M, the square covariance matrix is of order M.

The mean vector $\boldsymbol{\mu}$ is defined by

$$\boldsymbol{\mu} = \frac{1}{N} \sum_{i=1}^{N} \mathbf{x}^{(i)} \tag{2}$$

An n by m image can be represented as vector of dimension M ($M = nm$), that is a point in a large-dimension space. Therefore, the set of crop row images that represents all possible combinations of offset and heading angle could be discretized into N points and considered as a set of vectors $\mathbf{x}^{(1)}, \mathbf{x}^{(2)}, \ldots, \mathbf{x}^{(N)}$. Since the crop row images are highly correlated with each other, they are not randomly distributed in this M dimension image space. Thus, the PCA method was used to find a lower-dimensional subspace that was spanned by the eigenvectors that best account for the distribution of the N original images.

The matrix R presents a total of M eigenvectors with their M associated eigenvalues. The eigenvectors associated with the greatest eigenvalues are those that best account for the distribution. However, since there are N vectors in the original set, there will be N-1 eigenvectors with associated eigenvalues different from zero. In other words, the rest of the eigenvectors are not meaningful for PCA because their associated eigenvalues are zeros (Turk & Pentland, 1991).

Each image vector can be accurately reconstructed by a linear combination of the eigenvectors:

$$\mathbf{x}^{(i)} = a_1\mathbf{e}^{(1)} + a_2\mathbf{e}^{(2)} + \cdots + a_{N-1}\,\mathbf{e}^{(N-1)} + \boldsymbol{\mu} \tag{3}$$

where the $\mathbf{e}^{(i)}$ ($i = 1, 2, \ldots, N-1$) are the eigenvectors and the point $\mathbf{a}^{(i)} = (a_1, a_2, \ldots, a_{k-1})$ is the projection of the image $x^{(i)}$ into the eigenspace.

The eigenspace spanned by the eigenvectors $\mathbf{e}^{(i)}$ ($i = 1, 2, \ldots, N-1$) can be seen as a subspace with dimension equal to $N-1$ that precisely represents our scene of interest, *i.e.* the crop rows. However, since it is not necessary to have a precise reconstruction of the scene, the K ($K < N-1$) eigenvectors with the largest associated eigenvalues can be used in places of the $N-1$ eigenvectors. Thus, a faster algorithm that determines the first N greatest eigenvalues and their associated eigenvectors could be used (Murakami & Kumar, 1982).

The Euclidean distance between two points is a well-known parameter that can be used to determine the similarity between two images. Murase and Nayar (1995) showed that the square of the Euclidean distance between two points (images) in the original space is approximately equal to that between their projection into the N-dimensional eigenspace. Thus, determining the similarity between two images is reduced to a distance and projection problem.

4. Offset and heading angle detection algorithm

An algorithm to provide the guidance parameters from a crop row image was developed. It approached guidance parameter determination as 'pose' determination problem where each combination of offset and heading angle forms a 'pose'. It consisted of two parts: *training* based on *a priori* set of known pose images and *detection* based on an unknown pose image. Training generated a lower-dimensional eigenspace based on PCA. Detection stage output the heading angle and offset presented in an unknown pose image.

The eigenspace was generated from a set of training images with known offset and heading angle. A region of interest (ROI), rather than the whole image, was used as the variable $\mathbf{x}^{(i)}$ to generate the eigenspace and the effect of the position of the ROI was studied.

The row crop images were assumed to be adequately represented by the number of eigenvalues K that represented 80% of the variation of a scene,

$$\frac{\sum_{i=1}^{K} \lambda_i}{\sum_{j=1}^{N} \lambda_j} > 80 \tag{4}$$

where λ_i is the eigenvalue associated with the eigenvector $\mathbf{e}^{(i)}$.

Two kinds of eigenspaces were generated: the *global* and the *heading angle eigenspaces*. In some previous tests at the beginning of this research, using just a global eigenspace that represented all combinations of offset and heading angle, the algorithm estimated much better the heading angle than the offset of the vehicle. Thus, it was thought that the use of the heading angle eigenspaces could improve the algorithm performance. The heading angle eigenspaces was a subset of eigenspaces in each of them represented a different heading angle.

In detection, given a crop row image with unknown pose, the image was first projected onto the global eigenspace. The Euclidean distances between the projection and the projection of each training image was evaluated. The training image that presented the minimum distance was considered the first estimation of the guidance parameters. To improve the first estimation, the distance between the input image and three heading angle eigenspaces were determined. The three heading angle eigenspace were the first angle estimation, one below and another above the first estimation. The angle that presented the minimum distance was considered the final heading angle. To determine the final offset, the input image was projected onto the final heading angle

Table 1
The set of the test images (I) with the offset (O) and heading angle (HA) values*

I	*O*, *cm*	*HA*, *deg*	*I*	*O*, *cm*	*HA*, *deg*	*I*	*O*, *cm*	*HA*, *deg*	*I*	*O*, *cm*	*HA*, *deg*
1	+ 1·3	− 2	**13**	− 7·6	− 10	**25**	+ 9·0	+ 1	**36**	0·0	− 9
2	+ 2·3	− 2	**14**	− 8·7	− 10	**26**	+ 9·0	+ 3	**37**	+ 1·3	+ 17
3	− 7·6	− 2	**15**	− 8·0	− 10	**27**	+ 9·0	− 17	**38**	+ 1·3	+ 3
4	− 8·7	− 2	**16**	+ 0·3	0	**28**	+ 9·0	− 19	**39**	+ 2·3	+ 17
5	− 8·0	− 2	**17**	+ 0·7	0	**29**	+ 5·0	+ 1	**40**	+ 2·3	+ 3
6	+ 1·3	+ 18	**18**	− 7·3	0	**30**	+ 5·0	+ 3	**41**	− 7·6	+ 17
7	+ 2·3	+ 18	**19**	− 8·3	0	**31**	+ 5·0	− 17	**42**	− 7·6	+ 3
8	− 7·6	+ 18	**20**	− 8·0	0	**32**	+ 5·0	− 19	**43**	− 8·7	− 15
9	− 8·7	+ 18	**21**	+ 1·0	+ 1	**33**	0·0	+ 1	**44**	− 8·7	− 5
10	− 8·0	+ 18	**22**	+ 1·0	+ 3	**34**	0·0	− 1	**45**	− 8·0	− 15
11	+ 1·3	− 10	**23**	+ 1·0	− 17	**35**	0·0	+ 19	**46**	− 8·0	− 5
12	+ 2·3	− 10	**24**	+ 1·0	− 19						

* Positive was defined as right, negative was defined as left.

eigenspace and the square of Euclidean distance between its projection and the training image was used to make the final decision in the same way as the first estimation.

The training stage is computationally intensive. However, it is performed off-line and only once for a fixed camera setting. The pose determination stage involves a projection of a vector onto a subspace and determining the Euclidean distance between the projection of the input and the training set images. The projection is a dot product of an image with the K significant eigenvectors. Computational time is reduced from complete image reconstruction since K is selected to be much less than the total number of eigenvectors N. According to Tou & Gonzalez (1974), the search for the minimum Euclidean distance is equivalent to search for the maximum of

$$d_i(\mathbf{a}) = \mathbf{a}^T \mathbf{p}_i - \frac{1}{2}\,\mathbf{p}_i^T \mathbf{p}_i \qquad (5)$$

where $d_i(\mathbf{a})$ $(i = 1, 2, \ldots, N)$ is the decision function, $\mathbf{a}$ is the projection point of known pose and $\mathbf{p}_i$ is the projection of the ith training image. The second term is a constant for each $\mathbf{p}_i$ and can be determined off-line during the training set.

Both projecting and decision function processes have been implemented in real time by others (Turk & Pentland, 1991; Murase & Nayar, 1995). Additionally, the matrix form of this methodology well suited for parallel processing.

5. Experiment design

The algorithm was implemented in *MATLAB* (The MathWorks Inc, MA) and, since the main objective of this research was to evaluate the potential of the use of PCA to extract the vehicle guidance parameters, its performance was evaluated using a controlled environment and artificial lines representing crop rows. Artificial crop rows were painted on the laboratory floor and controlled illumination was used to acquire the images representing crop rows from different heading angle and offset positions. The image capture system consisted of a monochrome COHU model 4812 camera connected to an ImagiNation CX-100 frame grabber. The CX-100 board was set up to grab the images in high-resolution mode (512 pixel horizontally by 486 pixel vertically) with 8-bit pixels (256 grey levels). A 16 mm focal length lens was used with the camera.

For the training part of the algorithm, 231 images were collected. The heading angle was varied through a range of -20 to 20° in 2° increments. For each heading angle, 11 offset configurations were used: 0·0, 1·0, 3·0, 5·0, 7·0 and 9·0 cm (left and right). The camera was set on the top of a survey tripod to vary the heading angle; the camera tilt angle was 15°. The camera height was 0·80 m. The offset variation was done by changing the tripod position.

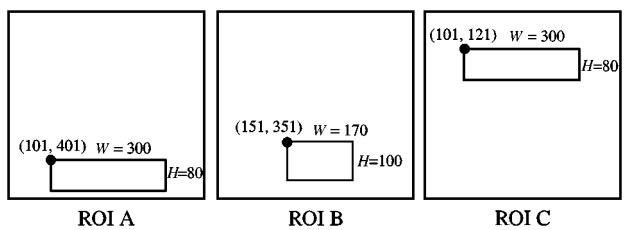

Fig. 1. Scheme of the regions of interested (ROI) used to test the algorithm showing their relative position within the whole image, left top pixel coordinate, width (W) and height (H) in pixels

Table 2
The tests run to test the algorithm

Test	*ROI* used to generate the global eigenspace*	*ROI* used to generate the heading angle eigenspaces*	*Test*	*ROI* used to generate the global eigenspace*	*ROI* used to generate the heading angle eigenspaces*
A	A	none	**BA**	B	A
B	B	none	**BB**	B	B
C	C	none	**BC**	B	C
AA	A	A	**CA**	C	A
AB	A	B	**CB**	C	B
AC	A	C	**CC**	C	C

* ROI, region of interest.

A global eigenspace was generated using all 231 training images. Twenty-one heading angle eigenspaces were generated, each one containing 11 training images from a particular heading.

In order to test the algorithm, 46 images were collected with different combinations of offset and heading angle from those used in the training part (Table 1). Three different rectangular ROIs were used to study how different image positions of pose information influenced the algorithm performance (*Fig. 1*). Thus, 12 different ROI configurations were used to generate the global and the heading angle eigenspaces (Table 2). Each of them was

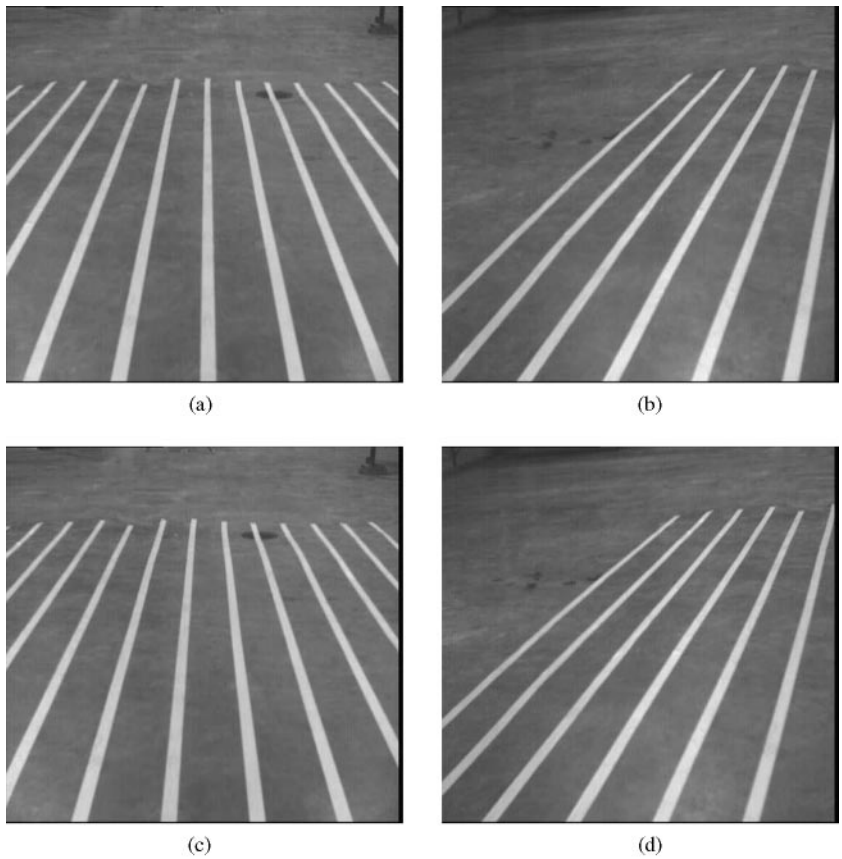

Fig. 2. Four images of the training set. (a) offset = 0·0 cm, and angle = 0°; (b) offset = 0·0 cm, and angle = − 18°; (c) offset = + 9·0 cm, and angle = 0°; (d) offset = + 9·0 cm, and angle = − 18°

Table 3
The offset and heading angle average μ, standard deviation σ, maximum (max) and minimum (min) absolute error for the experiments

Test	*Offset error, cm*				*Angle error, deg*			
	μ	σ	*max*	*min*	μ	σ	*max*	*min*
A	5·43	5·03	15·7	0·0	1·26	1·07	4	0
B	4·47	4·14	16·6	0·0	1·26	1·89	4	0
C	6·24	4·46	16·6	0·0	11·04	10·79	30	1
AA	5·05	4·66	16·7	0·0	1·35	1·13	4	0
AB	4·59	4·59	17·7	0·0	1·17	1·01	4	0
AC	5·69	4·12	17·7	0·0	1·83	1·03	4	0
BA	5·30	4·63	18·0	0·0	1·26	0·99	4	0
BB	4·60	4·54	18·0	0·0	1·26	1·03	4	0
BC	6·19	4·60	18·0	0·0	1·65	0·98	4	0

labelled with the ROI used. For example, test AB meant that the ROI A was used to generate the global eigenspace and ROI B was used to generate the heading angle eigenspaces. The absolute error between the actual offset and heading angle values and those output by the program were used as the measured performance parameter.

6. Results and discussion

Fig. 2 shows a sample of four images of the training set. The top row images present zero offset and the bottom ones present 9·0 cm right offset. The left column images present zero heading angle and the right ones present 18° left heading angle. Thus, horizontally, they represent the same offsets and, vertically, the same heading angle.

In Table 3, the overall statistics of the absolute error between the actual and the output algorithm values of the test images are presented.

The goal of the heading angle eigenspaces was to improve the estimation of the offset when the algorithm presents a 'good' first estimation for the heading angle in the global eigenspace. As it can be see in Table 3, because the algorithm did not present satisfactory estimation of the heading angle when using ROI C (test C), it did not make sense to run the tests for the heading angle eigenspaces related with this ROI (tests CA, CB and CC).

The dimensions of the global eigenspace for the ROI A, B and C were determined to be 15, 17 and 35, respectively, to represent 80% of the image variation. The dimensions of the heading angle eigenspaces alternated between 4 and 5. These numbers confirmed the effectiveness of PCA at reducing the space dimension that represents the scene. Eigenspace dimension and the algorithm performance in the field on row crops will be further explored to account for crop variations, illumination and other factors.

All of the experiments except test C had an average absolute error less than the 2° precision used in the training image set, therefore the algorithm was generally able to accurately estimate the heading angle. However, the algorithm offset estimation was above the 2 cm precision used in the training image set. *Figures 3–5* show the absolute error values for all 46 test images of the three

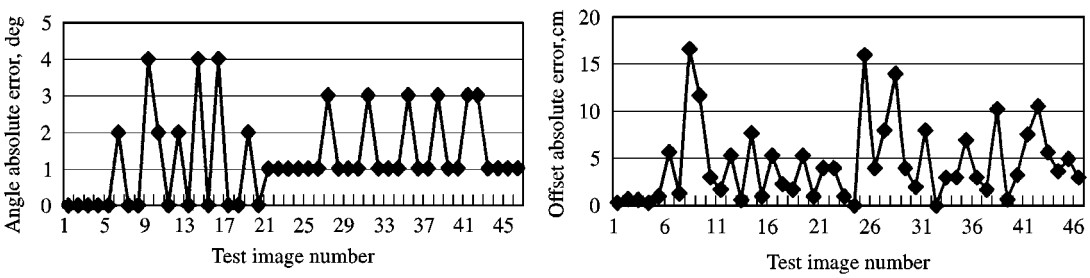

Fig. 3. The offset and heading angle absolute errors for all test images of the Test B

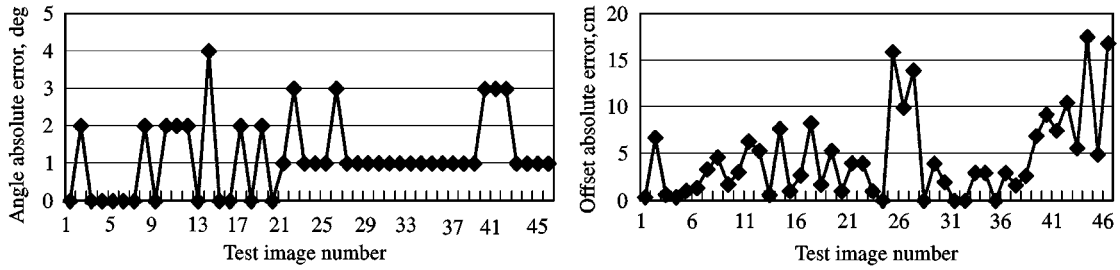

Fig. 4. The offset and heading angle absolute errors for all test images of the Test AB

tests that presented the lowest average absolute offset (tests B, AB and BB).

In *Fig. 6*, three images with the same offset and three consecutive heading angles are displayed together. It was noted that they presented two regions where the rows overlapped. Comparing *Figs 6a* with *b*, it was noted that the size and position of the overlapping regions changed depending on the offset and the heading angle of the scene. This property of the row scenes could be one of explanation about the ROI influence on the performance of the algorithm. It also suggests that the use of an adaptive ROI could improve the algorithm performance.

7. Conclusions

In this research, the vehicle offset and the heading angle extraction from the image for automatic guidance purposes was addressed as a 'pose recognition' problem. A set of 231 known pose images was collected and used as a training set. The training stage of the algorithm used the principal component analysis (Hotelling transform) to output two low-dimensional eigenspaces, the global and the heading angle eigenspaces. The poses were represented on these eigenspaces by their projections. Given a new image, the pose (heading angle and offset) recognition algorithm would project the image onto the eigenspace and determine the pose based on the closest training image projection.

The algorithm was tested with three different regions of interests (ROI) by using 46 known pose test images. Thus, 12 different combinations of these ROI were used to generate the global and the heading angle eigenspaces. The algorithm presented satisfactory performance for estimating heading angle. The best result was reached when the central ROI was used without the heading angle eigenspace. In this test, the algorithm presented the average absolute error of 4·47 cm and 1·26° for offset and heading angle, respectively. Additional research is needed to understand the influence of ROI size and position and the relationship between the offset and the heading angle influence on algorithm performance in order to improve the offset estimation.

Acknowledgements

This research was sponsored by the University of Illinois Research Board and the Council for Food and Agricultural Research (Project No. 1595198). The first author has been sponsored by the Brazilian Agency CAPES.

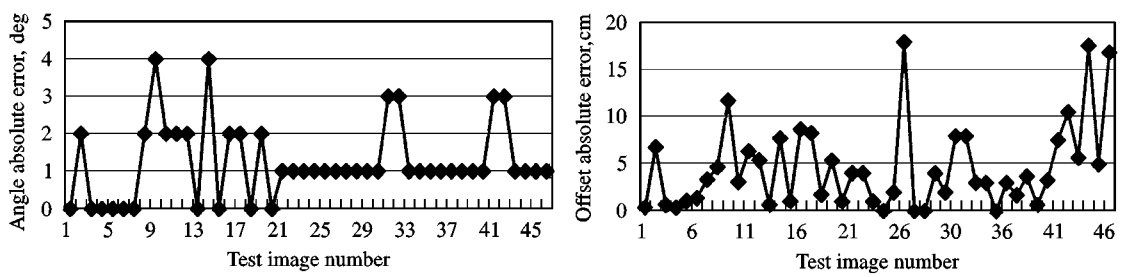

Fig. 5. The offset and heading angle absolute errors for all test images of the Test BB

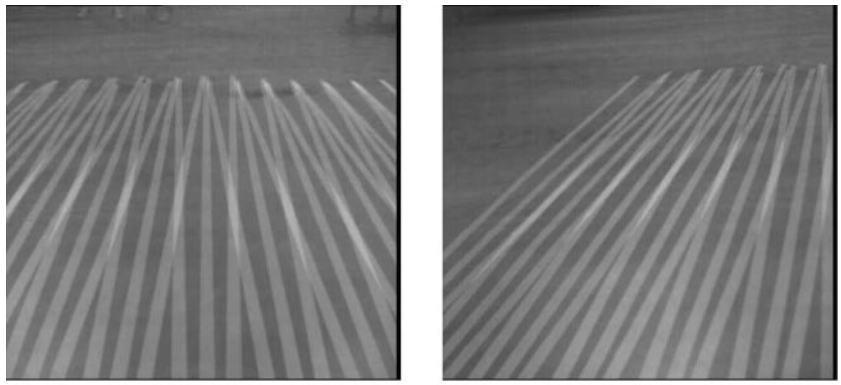

Fig. 6. Three images with the same of offset and three consecutive heading angles displayed together. (a) offset = 0·0 cm, and angles = − 2, 0 and + 2°. (b) offset = 0·0 cm, and angles = − 14, − 16 and − 18°

References

Ahmad I S; Reid J F (1996). Evaluation of colour representations for maize images. Journal of Agricultural Engineering Research, **63,** 185–196

Billingsley J; Schoenfish M (1997). The successful development of a vision guidance system for agriculture. Computers and Electronics in Agriculture, **16,** 147–163

Gerrish J B; Stockman G; Mann L; Hu G (1987). Path-finding by image processing in agricultural field operation. Transactions of the SAE, **95**(5), 540–554

Gonzalez R C; Woods R E (1992). Digital Image Processing. Addison-Wesley Publishing Company, Reading, MA

Hotelling H (1933). Analysis of a complex of statistical variables into principal components. The Journal of Educational Psychology

Isebrands J G; Crow T R (1975). Introduction to uses and interpretation of principal component analysis in foresty biology. USDA Forest Service General Technical Report NC-17

Jolliffe I T (1986). Principal Component Analysis, Springer Series in Statistics. Springer-Verlag, New York Inc., NY

Kirby M; Sirovich L (1990). Application of the Karhunen–Loeve procedure for the characterization of human faces. IEEE Transactions on Pattern Analysis and Machine Intelligence, **12**(1), 103–108

Murakami H; Kumar V K (1982). Efficient calculation of primary images from a set of images. IEEE Transactions on Pattern Analysis and Machine Intelligence, **4**(5), 511–515

Murase H; Nayar S K (1995). Visual learning and recognition of 3-D objects from appearance. International Journal of Computer Vision, **14,** 5–24

Noguchi N; Ishii K; Terao H (1997). Development of an agricultural mobile robot using a geomagnetic direction sensor and image sensors. Journal of Agricultural Engineering Research, **67,** 1–15

Noguchi N; Reid J F; Zhang Q; Tian L F (1998a). Vision intelligence for precision farming using fuzzy logic optimized genetic algorithm and artificial neural network. ASAE Paper No 98–3034

Noguchi N; Reid J F; Will J; Benson E R; Stombaugh T S (1998b). Vehicle automation system based on multisensor integration. ASAE Paper No 98–3111

Reid J F (1987). The development of computer vision algorithms for agricultural vehicle guidance. Unpublished PhD thesis Texas A and M University, College Station, TX

Slaughter D C; Chen P; Curley R G (1997). Computer vision guidance system for precision cultivation. ASAE Paper No 97–1079

Steward B; Tian L F (1998). Real-time machine vision weed sensing. ASAE Paper No 98–7006

Tou J T; Gonzalez R C (1974). Pattern Recognition Principles. Addison-Wesley Publishing Company, Reading, MA

Tillet N D (1991). Automatic guidance sensors for agricultural field machines: a review. Journal of Agricultural Engineering Research, **50,** 167–187

Turk M; Pentland A (1991). Eigenfaces for recognition. Journal of Cognitive Neuroscience, **3**(1), 71–86

Von Qualen K E; Hummel J M; Reid J F (1991). Machine vision system for field sprayer guidance. In: Proceedings of the Automated Agriculture for the 21st Century, pp 192–200